Published in final edited form as:

Science. 2023 September 08; 381(6662): 1072–1079. doi:10.1126/science.adg9232.

Oxidative addition of an alkyl halide to form a stable Cu(III) product

Yongrui Luo[1,†], **Yuli Li**[1,†], **Jian Wu**[1], **Xiao-Song Xue**[1,*], **John F. Hartwig**[2,*], **Qilong Shen**[1,*]

[1]Key Laboratory of Organofluorine Chemistry, Center for Excellence in Molecular Synthesis, Shanghai Institute of Organic Chemistry, University of Chinese Academy of Sciences, Chinese Academy of Sciences, Shanghai 200032, PR China.

[2]Department of Chemistry, University of California, Berkeley, Berkeley, CA 94720, USA.

Abstract

The step that cleaves the carbon-halogen bond in copper-catalyzed cross-coupling reactions remains ill defined because of the multiple redox manifolds available to copper and the instability of the high-valent copper product formed. We report the oxidative addition of α-haloacetonitrile to ionic and neutral copper(I) complexes to form previously elusive but here fully characterized copper(III) complexes. The stability of these complexes stems from the strong Cu–CF_3 bond and the high barrier for C(*CF_3*)–C(*CH_2CN*) bond-forming reductive elimination. The mechanistic studies we performed suggest that oxidative addition to ionic and neutral copper(I) complexes proceeds by means of two different pathways: an S_N2-type substitution to the ionic complex and a halogen-atom transfer to the neutral complex. We observed a pronounced ligand acceleration of the oxidative addition, which correlates with that observed in the copper-catalyzed couplings of azoles, amines, or alkynes with alkyl electrophiles.

Editor's summary

Copper-mediated couplings are among the oldest reactions in organic chemistry. Nonetheless, their mechanisms still are not as predictably well understood as those of the palladium catalysts that came later. Part of the difficulty is tracking the one-electron increments through which copper typically reacts, shuffling between the +1 and +2 oxidation states. Two studies now uncover two-electron processes at play instead. Delaney *et al.* found that ligand oxidation enables oxidative addition of an aryl halide to Cu(II), avoiding the need for a less stable Cu(I) precursor. Luo *et al.* observed halonitrile addition to Cu(I) complexes to produce isolable Cu(III). Both results point to future innovative catalyst optimization strategies. —Jake S. Yeston

[*]**Corresponding author.** xuexs@sioc.ac.cn (X-S.X.); jhartwig@berkeley.edu (J.F.H.); shenql@sioc.ac.cn (Q.S.).
[†]These authors contributed equally to this work.

Author contributions: Y. Luo performed the experiments and analyzed experimental data. Y. Li performed the DFT calculations. J.W. assisted in the kinetic studies. X.-S.X., J.F.H., and Q.S. directed the research. Y. Luo, J.F.H., and Q.S. wrote the manuscript.

Competing interests: The authors declare that they have no competing interests.

Data materials and availability: Crystallographic data are available free of charge from the Cambridge Crystallographic Data Centre (CCDC) under CCDC 2236874 (**3a**), 2236875 (**3b**), and 2236887 (***trans*-4**). All other data reported in this paper are available in the manuscript or the supplementary materials.

Copper-mediated cross-coupling reactions have become some of the most powerful methods for the construction of carbon-carbon (C–C) and C–heteroatom bonds (1–4). Early efforts in this field focused mainly on the coupling of sp^2-hybridized carbon electrophiles, and in recent years, research has expanded to encompass the mild coupling of sp^3-hybridized carbon electrophiles (5, 6). Much progress has been made recently on copper-mediated or copper-catalyzed alkynylation (7–9), alkylation (10–12), arylation (13–15), and amination (16, 17) of alkyl halides, providing an alternative and practical method for the installation of functional groups on alkyl chains and rings. Despite this expansion of the scope of the cross-coupling reactions of alkyl electrophiles that use copper, the mechanism of these reactions is poorly understood.

Previously, two distinct cycles were proposed for copper-catalyzed cross-coupling reactions of alkyl electrophiles. One cycle comprises a two-electron Cu(I)/Cu(III) manifold, and one comprises a stepwise Cu(I)/Cu(II) manifold involving initial single-electron transfer (SET) between the Cu(I) center and the alkyl electrophile to generate a Cu(II) intermediate and an alkyl radical, followed by transfer of the functional group from the resulting Cu(II) species to the alkyl radical (18–22) (Fig. 1A). Differentiation of these two pathways is challenging because the higher-valent copper intermediates in the reactions, particularly the putative Cu(III) intermediates, are highly reactive and typically elude detection (23–26).

Consequently, isolable, well-defined alkyl Cu (III) complexes are rare. In the early 2000s, seminal work from the groups of Bertz, Ogle (27–29), and Gschwind (30) demonstrated that reactions of alkyl iodides with ionic Gilman reagents generated Cu(III) species, which were characterized at a temperature below −93°C with rapid-injection nuclear magnetic resonance (RI-NMR) spectroscopy techniques (Fig. 1C). Yet, formation of the Cu(III) intermediates, even at this temperature, is fast, rendering studies on the mechanism of the reaction of alkyl halides with the Cu(I) species challenging.

To probe whether a Cu(III) intermediate could be generated from the reaction of an alkyl halide with a Cu(I) species and to determine how such an intermediate would form from an alkyl electrophile in a copper-mediated or copper-catalyzed cross-coupling, we reasoned that two requirements must be met: (i) An alkyl electrophile with a high reduction potential must be used so that formation of the Cu(III) species from the starting Cu (I) species is thermodynamically favorable, and (ii) the barrier for reductive elimination from the Cu(III) intermediate must be higher than that for the oxidative addition that forms the Cu(III) species (Fig. 1B).

The electron-withdrawing, strong-field trifluoromethyl ligand is known to stabilize both Cu(I) and high-valent Cu(III) metal centers as a result of π-back donation of electron density from the d orbitals on copper to the antibonding (σ*) orbitals of the C–F group or the contracted bonding (σ) orbitals on copper because of the high electronegativity of the fluorine (31). In the past three decades, a variety of well-defined trifluoromethyl Cu(III) complexes have been reported (26). Recent studies on the reactivities of these Cu(III) complexes showed that the barrier for reductive elimination to form a $C(sp^3)–CF_3$ bond from either the ionic Cu(III) complex $[Cu(CF_3)_3(alkyl)]^-$ or the five-coordinate neutral Cu(III) complex $[(bpy)Cu(CF_3)_2(Me)]$ is high (32–34). In addition, stable, well-characterized

trifluoromethyl Cu(I) species—including [$CuCF_3$] (35), which contains no additional ligands; [(Phen)$CuCF_3$] (36), which contains a dinitrogen-donor ligand; [(NHC)$CuCF_3$] (37), which contains an *N*-heterocyclic carbene (NHC) ligand; and [$Cu(CF_3)_2]^-$ (38, 39), which is an ionic Cu(I) cuprate—were reported to react with aryl halides to give trifluoromethylarene products in good yields. In light of this prior work, we proposed that an appropriate trade-off between reactivity and stability of trifluoromethyl Cu(I) and Cu(III) complexes could meet the aforementioned requirements and provide an opportunity to investigate the mechanism of the reaction of alkyl halides with Cu(I) species to form stable Cu(III) products.

On the basis of the above rationale, we studied the reactions of alkyl halides with trifluoromethyl-Cu(I) complexes (Fig. 1). Stable $[Ph_4P]^+[Cu(CF_3)_2]^-$ and [(bpy)$Cu(CF_3)$] (bpy, bipyridine) were chosen initially as the Cu(I) complexes that represent the ligandless "ate"-type Cu(I) complex and the neutral bipyridine-ligated Cu(I) complex, respectively. These complexes would allow us to probe the differences between the reactivity of two different types of Cu(I) complexes and the effect of the nitrogen ligand on the oxidative addition process. We chose α-haloacetonitrile XCH_2CN [in which X (halogen) is Cl, Br, or I] as the alkyl electrophile because XCH_2CN is more electrophilic than other alkyl halides, reducing the barrier for oxidative addition to Cu(I). In addition, because of the electron-withdrawing property of the cyano group, the barrier for C–C bond-forming reductive elimination from a [(ligand)$Cu^{III}(CF_3)_2(CH_2CN)$] complex could be sufficiently high for the product to be observed directly and possibly isolated. We report the isolation of Cu(III) complexes from oxidative addition of haloacetonitrile to ionic and neutral trifluoromethyl Cu(I) complexes. Mechanistic investigation of these reactions, conducted with a combination of computational and experimental studies, shows that anionic and neutral complexes react with the same alkyl halide by means of distinct mechanisms.

Isolation and characterization of Cu(III) products

We initially studied the reactions of $[Ph_4P]^+$ [Cu(CF3)2]$^-$ (**1a**) or a neutral Cu(I) complex [(bpy)$Cu(CF_3)$] (**1b**) with haloacetonitriles $ClCH_2CN$ (**2-Cl**), $BrCH_2CN$ (**2-Br**), and ICH_2CN (**2-I**) or alkyl tosylate $TsOCH_2CN$ (**2-OTs**) (Fig. 2A). The reaction of 2.0 equivalents of anion **1a** and bromide **2-Br** in dimethyl sulfoxide (DMSO) occurred smoothly at room temperature after 3.0 hours to give two previously unknown species in an approximate 1:1 ratio in quantitative yield, as determined by ^{19}F NMR spectroscopy. One species, corresponding to chemical shifts of −33.4 and −34.4 parts per million (ppm) in a 1:2 integral ratio in the ^{19}F NMR spectrum, was assigned as the tetracoordinate ionic Cu(III) complex $[Ph_4P]^+[Cu(CF_3)_3(CH_2CN)]^-$ (**3a**) (fig. S1). Cu(III) complex **3a** was stable enough to be isolated and characterized by ^1H, ^{19}F, and ^{31}P NMR spectroscopies and elemental analysis. The structure of complex **3a** was further confirmed by single-crystal x-ray diffraction, which revealed a typical square-planar geometry (Fig. 2C, top). The second complex, corresponding to a chemical shift at −27.0 ppm in the ^{19}F NMR spectrum, was assigned as a cuprate(I) species, $[Ph_4P]^+[Cu(CF_3)(Br)]^-$ (**1c**). We presume that complexes **3a** and **1c** were generated from transmetalation of the oxidative addition product $[Ph_4P]^+$ $[Cu(CF_3)_2(CH_2CN)(Br)]^-$ with Cu(I) complex $[Ph_4P]^+[Cu(CF_3)_2]^-$ (**1a**). It was found that complex **1c** was much less reactive than complex **1a**. It reacted with 1.0 equivalent of

bromide **2-Br** in DMSO, resulting in 30% conversion and 9% yield of **3a** after 3 hours at room temperature. Thus, the formation of bromocuprate **1c** does not affect the oxidative addition of **2-Br** to$[Ph_4P]^+[Cu(CF_3)_2]^-$ (**1a**). As did the reaction of bromide **2-Br**, the reaction of iodide **2-I** with cuprate **1a** occurred smoothly to give Cu(III) complex **3a** in more than 90% yield and $[Ph_4P]^+[Cu(CF_3)(I)]^-$ (**1d**) in 62% yield, respectively. By contrast, the reaction of chloride **2-Cl** with cuprate **1a** was much slower, and the starting materials remained intact even after 5 hours at room temperature (Fig. 2A). We also studied the reaction of tosylate **2-OTs** with **1a** and found that complex **1a** was fully converted within 3 hours at 25°C, but the yield for the formation of Cu(III) complex **3a** was much lower (15%) than those from the reactions of **2-Br** or **2-I** (Fig. 2A).

The reaction of neutral Cu(I) complex [(bpy) $Cu(CF_3)$] (**1b**) with $BrCH_2CN$ (**2-Br**) occurred much faster than that of ionic Cu(I) complex $[Ph_4P]^+[Cu(CF_3)_2]^-$ (**1a**). The reaction of **1b** with bromide **2-Br** in *N,N*-dimethylformamide (DMF)generated *trans*-[(bpy)$Cu(CF_3)_2(CH_2CN)$] (***trans*-4**) and *cis*-[(bpy)$Cu(CF_3)_2(CH_2CN)$] (***cis*-4**) in 56 and 4% yields, as well as [(bpy)CuBr], respectively, after just 1 min at room temperature (Fig. 2B). Complex ***trans*-4** was fully characterized by ^1H and ^{19}F NMR spectroscopies, as well as elemental analysis.

X-ray diffraction of the single crystal of ***trans*-4** shows that it adopts a distorted square-pyramidal geometry. The H_2C–Cu–N angle to the apical nitrogen is 121.9°, and that to the equatorial nitrogen is 160.2°; the length of the N–Cu bond at the apical position (2.236 Å) is considerably longer than that of the N–Cu bond in the equatorial position (1.987 Å), indicating that the geometry is closer to a square-based pyramid than a trigonal bipyramid (Fig. 2C, bottom).

Reaction of complex **1b** with iodide **2-I** also occurred quickly to give ***trans*-4** and ***cis*-4** in 67 and 11% yields, respectively, under similar conditions (Fig. 2B). In contrast to cuprate **1a**, the neutral complex **1b** reacted with chloride **2-Cl** to give ***trans*-4** in 49% yield at room temperature after just 1 hour (Fig. 2B). These rapid rates indicate that the neutral Cu(I) complex **1b** is much more reactive toward the alkyl halide than is ionic Cu(I) complex **1a**, reflecting a sizable ligand acceleration (Fig. 2D). Such a phenomenon has previously been observed in various copper-mediated or -catalyzed cross-coupling reactions (40, 41).

The large difference in reactivity of ionic and neutral Cu(I) complexes led us to conduct reactions that would reveal the mechanisms by which the two complexes react with alkyl halides. The reaction of bromide **2-Br** with ionic Cu(I) complex $[Ph_4P]^+$ $[Cu(CF_3)_2]^-$ (**1a**) was sensitive to the polarity of the solvent. The reactions conducted in polar solvents, such as DMSO, *N,N*-dimethylacetamide (DMAc), and DMF, proceeded to 96, 87, and 76% conversion at room temperature over 5 hours and afforded Cu(III) complex **3a** in 93, 70, and 60% yields, respectively (table S1), whereas the same reactions in less-polar solvents, such as tetrahydrofuran (THF) or CH_2Cl_2, occurred more slowly (24 and 12% conversions after 5 hours at room temperature) to give complex **3a** in just 13 and 11% yields, respectively (Fig. 2E). By contrast, the reaction of chloride **2-Cl** or bromide **2-Br** with the neutral Cu(I) complex [(bpy)Cu(CF3)] (**1b**) was not sensitive to the polarity of the solvent. Reactions of complex **1b** with chloride **2-Cl** in the more-polar solvent DMF or the less-polar solvent

THF occurred to full conversion after 1 hour at room temperature to afford Cu(III) complex ***trans*-4** in 59 and 82% yields, respectively (Fig. 2E). Quantitative assessment of the reaction of chloride **2-Cl** with complex **1b** in THF and DMF at −5°C showed that the rates of the two reactions are similar [$(3.02 \pm 0.10) \times 10^{-3}$ $M^{-1}{\cdot}s^{-1}$ in THF and $(3.43 \pm 0.32) \times 10^{-3}$ $M^{-1}{\cdot}s^{-1}$ in DMF, respectively (fig. S25)]. The different sensitivities of the ionic and neutral Cu(I) species to solvent polarity indicate that these Cu(I) complexes might react with the alkyl halide through different mechanisms.

Kinetic studies

To investigate the effect of the properties of the C–X bond of the haloacetonitriles on the reactions with cuprate $[Ph_4P]^+[Cu(CF_3)_2]^-$ (**1a**) or neutral [(bpy)Cu(CF_3)] (**1b**), we compared the rates of reactions of **1a** or **1b** with XCH_2CN quantitatively by monitoring the ^{19}F NMR signals corresponding to **1a** for reaction of complex **1a** and the signals corresponding to ***trans*-4** and ***cis*-4** for the reaction of complex **1b**. These studies showed that reactions of the ate complex are first order in complex **1a** and first order in bromide **2-Br** (Fig. 3A and figs. S3 to S6). The reaction of complex **1a** with iodide **2-I** [$(8.54 \pm 0.04) \times 10^{-3}$ $M^{-1}{\cdot}s^{-1}$] was about five times as fast as that with bromide **2-Br** [$(1.78 \pm 0.03) \times 10^{-3}$ $M^{-1}{\cdot}s^{-1}$ at 25°C]. Because complex **1a** reacted with chloride **2-Cl** slowly at room temperature (Figs. 2A and 3A), we studied the reaction at elevated temperature. At 60°C, the reaction occurred with a rate constant of $(1.99 \pm 0.14) \times 10^{-4}$ $M^{-1}{\cdot}s^{-1}$. The rate constant for the reaction of complex **1a** with bromide **2-Br** at 60°C was estimated to be 4.05×10^{-2} $M^{-1}{\cdot}s^{-1}$ on the basis of the Eyring analysis in Fig. 3C, which is roughly 200 times as fast as that with chloride **2-Cl**.

The rates of the reactions of the halides with neutral complex **1b** were measured with ^{19}F NMR spectroscopy below room temperature because of their high rate. The reaction of bromide **2-Br** with [(bpy)Cu(CF_3)] (**1b**) at −30°C proceeded to full conversion after 20 min. Kinetic studies showed that this reaction is first order in both reactants and that the rate constant at −30°C is $(2.63{\pm}0.05){\times}10^{-2}$ $M^{-1}{\cdot}s^{-1}$. At this temperature after 5 min, the reaction of chloride **2-Cl** with [(bpy)Cu(CF_3)] (**1b**) proceeded to <1% conversion (Fig. 3B). However, the reaction of chloride **2-Cl** with complex **1b** at −5°C occurred with a rate constant of $(3.43 \pm 0.32) \times 10^{-3}$ $M^{-1}{\cdot}s^{-1}$. According to the Eyring analysis shown in Fig. 3C, the rate constant for reaction of complex **1b** with bromide **2-Br** at −5°C was estimated to be 0.37 $M^{-1}{\cdot}s^{-1}$, which is roughly 100 times greater than that of the reaction of complex **1b** with chloride **2-Cl**. The rate dependence of these reactions of the ionic and neutral Cu(I) species on the strength of the C–X bond and on the leaving group ability of the alkyl halidesis consistent with typicalCu(I)-catalyzed cross-coupling reactions.

To evaluate the effect of the steric properties of the alkyl bromide on the reaction of the Cu(I) complex, we studied the reaction of Cu(I) complex $[Ph_4P]^+[Cu(CF_3)_2]^-$ (1a) with the secondary alkyl halide, 2-bromopropionitrile **2-Br-Me**, and the tertiary alkyl halide, 2-methyl-2-bromopropionitrile **2-Br-Me_2** (Fig. 2A). Reaction of cuprate **1a** with 2-bromopropionitrile **2-Br-Me** occurred smoothly at room temperature over 5 hours to give Cu(III) complex **3b** in 81% yield. Yet, this reaction of the more sterically hindered 2-bromopropionitrile **2-Br-Me** was slower than that of the less-hindered bromoacetonitrile

2-Br [(1.15 ± 0.01) × 10^{-3} M^{-1}·s^{-1} versus (1.78 ± 0.03) × 10^{-3} M^{-1}· s^{-1}]. To determine whether the reactions of complex **1a** occurred with inversion of configuration, we conducted the reaction of **1a** with optically active (*R*)-2-bromopropionitrile (*R*)-**2-Br-Me**, but the enantiomers of the resulting product **3b** did not separate through chiral high-performance liquid chromatography (HPLC) column and only weakly absorbed in the ultra-violet, preventing assessment of the configuration of the product with chromatography or spectroscopy. The reaction of **1a** with the tertiary alkyl halide, 2-methyl-2-bromopropionitrile **2-Br-Me$_2$**, did not afford the corresponding Cu(III) complex from oxidative addition. Instead, Cu(III) complex $[Ph_4P]^+$ $[Cu(CF_3)_4]^-$ and Cu(I) complex $[Ph_4P]^+$ $[Cu(CF_3)(Br)]^-$ formed in 31 and 7% yields, respectively, as determined by ^{19}F NMR spectroscopy of the reaction mixture, as well as a few unidentified Cu(II) species, which were indicated by the color of the reaction mixture turning green. Analysis of the reaction mixture showed that isobutyronitrile **6** also formed through hydrodehalogenation. This observation suggests that the reaction forms the isobutyronitrile radical, which is too sterically hindered to combine with the trifluoromethyl Cu(II) species and, instead, abstracts a hydrogen atom from the solvent. The reaction of 2-chloropropionitrile **2-Cl-Me** with the neutral complex [(bpy)Cu(CF_3)] (**1b**) occurred over 1 hour at 25°C to generate the corresponding Cu(III) complex ***trans*-4b** in 12% yield. This complex was characterized with ^{19}F NMR spectroscopy because it was too unstable to be isolated.

Inhibition studies

To probe whether the oxidative additions of XCH_2CN to Cu(I) complexes $[Ph_4P]^+$ [Cu(CF3)2]$^-$ (**1a**) and [(bpy)Cu(CF_3)] (**1b**) occur by means of a radical intermediate and whether a potential radical would form through initial SET, we first studied the reaction in the presence of radical inhibitor 2,2,6,6-tetramethylpiperidine-1-oxyl (TEMPO) and in the presence of SET inhibitor 1,4-dinitrobenzene. The reaction of **1a** with $BrCH_2CN$ **2-Br** in the presence of 2.0 equivalents of TEMPO was complete after 3 hours at room temperature. The yield of this reaction (64%) was only 29% less than that in the absence of TEMPO, and only 19% of the radical adduct TEMPO−CH2CN **5** was isolated (Fig. 2A). By contrast, TEMPO had a strong effect on the reaction of **1b** with $ClCH_2CN$ **2-Cl**, resulting in the formation of ***trans*-4** in 10% yield and TEMPO-CH_2CN **5** in 75% yield (Fig. 2B). SET inhibitor 1,4-dinitrobenzene did not noticeably affect the reaction of haloacetonitrile with either the ionic Cu(I) complex **1a** or the neutral Cu(I) complex **1b**. These results suggest that alkyl radicals are generated in the oxidative addition of **1a** or **1b** with bromoacetonitrile but that a SET process is unlikely to lead to the radical in either case.

Effect of ligand

The bipyridine ligand in complex **1b** could in principle dissociate from the metal center to create a less sterically hindered intermediate that reacts with the alkyl halide. If reaction of $ClCH_2CN$ with neutral Cu(I) complex [(bpy)Cu(CF_3)] (**1b**) occurred through reversible dissociation of the bipyridine, addition of free bipyridine to the reaction should substantially reduce the rate. The reactions in the presence of varying amounts of bipyridine (3.0, 6.0, and 10.0 equivalents versus **1b**) occurred with nearly equal rate constants [(2.81 ± 0.01) × 10^{-3} M^{-1}·s^{-1}, (3.33 ± 0.21) × 10^{-3} M^{-1}·s^{-1}, and (2.91 ± 0.12) × 10^{-3} M^{-1}·s^{-1}, respectively] and

were only slightly slower than the reaction in the absence of added 2,2′-bipyridine [(3.61 ± 0.08) × 10^{-3} $M^{-1}{\cdot}s^{-1}$] (Fig. 3D). These data imply that reversible dissociation of the ligand does not precede rate-limiting oxidative addition to **1b**.

Activation parameters

To determine the enthalpy and entropy of activation of both reactions, we studied the effect of the temperature on the rates. An Eyring plot of ln(*k*/*T*) versus 1/*T* (where *k* is the rate constant and *T* is temperature) for the reaction of ionic Cu(I) complex $[Ph_4P]^+[Cu(CF_3)_2]^-$ (**1a**) with bromide **2-Br** between 25° and 37°C revealed an activation enthalpy, $\Delta H^{\ddagger}$, of 17.7 ± 0.4 kcal/mol and an activation entropy, $\Delta S^{\ddagger}$, of −12 ± 1 entropy units (e.u.) (Fig. 3C, blue). Likewise, an Eyring analysis of the reaction of neutral Cu(I) complex [(bpy)$Cu(CF_3)$] (**1b**) with **2-Br** over a temperature range of −30° to −20°C revealed an activation enthalpy, $\Delta H^{\ddagger}$, of 13.0 ± 0.6 kcal/mol and a similar activation entropy, $\Delta S^{\ddagger}$, of −12 ± 2 e.u. (Fig. 3C, green). The activation entropies of the reactions of **1a** and of **1b** with **2-Br** were similar, but the activation enthalpy for the reaction of **2-Br** with **1b** was much less than that with **1a**. An Eyring analysis of the reaction of [(bpy)$Cu(CF_3)$] (**1b**) with $ClCH_2CN$ (**2-Cl**) between −8° and 4°C revealed a $\Delta H^{\ddagger}$ of 15.2 ± 0.8 kcal/mol and a $\Delta S^{\ddagger}$ of −13 ± 3 e.u. (Fig. 3C, red), and this value for $\Delta H^{\ddagger}$ is similar to, or even slightly less than, that for oxidative addition of $BrCH_2CN$ (**2-Br**) to cuprate(I) complex $Ph_4P^+[Cu(CF_3)_2]^-$ (**1a**) (17.7 ± 0.4 kcal/mol), even though the C–Cl bond in $ClCH_2CN$ (**2-Cl**) (70.5 kcal/mol) is much stronger than the C–Br bond in $BrCH_2CN$ (**2-Br**) (56.8 kcal/mol) and the chloride is less polarizable and is a poorer leaving group than bromide (42).

To define the mechanism of the reaction of haloacetonitrile with the ionic or neutral Cu(I) species further, we performed density functional theory (DFT) calculations with the PBE0-D3(BJ) functional. On the basis of previous proposals for the mechanism of copper-mediated cross-coupling reactions (18–22) and the experimental results reported in this work, we proposed five different pathways that could account for the oxidative addition of haloacetonitrile to ionic and neutral Cu(I) complexes (Fig. 4). The first pathway (pathway A) involves an S_N2 step and is a common type of two-electron oxidative addition of alkyl halides to late transition metals, such as Pt (43) and Pd (44). In addition, such a pathway was proposed by Whitesides (45) and Pearson (46) for the reaction of lithium dialkylcuprates with alkyl halides (the Corey-Posner reaction) to generate a Cu(III) intermediate, which would then undergo fast reductive elimination to form the C–C bond in the product. In our case, reaction of **1a** through this mechanism would form Cu(III) species $[Cu^{III}(CF_3)_2(CH_2CN)]$ or $[Ph_4P]^+[Cu^{III}(CF_3)_2(X)(CH_2CN)]^-$, which would then undergo transmetalation with **1a** to generate $[Ph_4P]^+[Cu^{III}(CF_3)_3(CH_2CN)]^-$ (**3a**) and $[Cu(CF_3)X]^-$. Likewise, reaction with **1b** would give $[(bpy)Cu^{III}(CF_3)(CH_2CN)]^+$ or [(bpy)Cu^{III} $(CF_3)(X)(CH_2CN)$], which would undergo transmetalation with **1b** to give [(bpy)$Cu^{III}(CF_3)_2(CH_2CN)$] (***trans*-4** or ***cis*-4**) and [(bpy)CuX], respectively (details about transmetalation are provided in fig. S31). A second two-electron mechanism for oxidative addition would be a concerted addition of the C–X bond to the metal center (pathway B), and this step would be the reverse reaction of concerted reductive elimination from a high-valent Cu center. A third pathway for oxidative addition of alkyl halides to a Cu(I) center could

occur through consecutive single-electron steps. One commonly proposed mechanism for oxidative addition through single-electron steps is outer-sphere SET (OSET; pathway C), which dominates the redox manifolds of first-row transition metals, including Fe (47) and Ni (48). A fourth pathway and an alternative mechanism for oxidative addition through single-electron steps is halogen-atom transfer (XAT; pathway D) (49, 50). Ligated Cu(I) complexes are widely used in atom-transfer radical addition or polymerization (ATRA or ATRP) processes in which a XAT to Cu is involved (51). A fifth pathway, oxidative addition of the alkyl halide to Cu(I), could occur by initial ligand dissociation to generate a neutral, ligandless [$CuCF_3$], which would undergo oxidative addition of the alkyl halide to generate a Cu(III) intermediate that would recoordinate the dative ligand and undergo transmetalation to give the final Cu(III) complex (pathway E) (52). The energy parameters for these pathways were computed and are shown in Fig. 4. In all five proposed mechanistic pathways, the formation of final product **3a** from the reaction of **1a** and the formation of ***trans*-4/*cis*-4** from reaction of **1b** involve a transmetalation step after initial formation of a Cu(III) complex. The absence of observed intermediates before transmetalation and first-order rate behavior in the Cu(I) species (**1a** or **1b**) rule out both rate-limiting transmetalation for these reactions and the initial generation of the Cu(III) intermediate through reaction of two copper complexes.

Evidence for XAT and S_N2 pathways

On the basis of the experimental results and DFT calculations, we concluded that reaction of the ionic Cu(I) complex $[Ph_4P]^+[Cu(CF_3)_2]^-$ (**1a**) with $BrCH_2CN$ (**2-Br**) likely proceeds by means of two different pathways, specifically the major fraction through an S_N2-type process (pathway A) and the minor fraction through a XAT process (pathway D). We also conclude that the reaction of the neutral Cu(I) complex [(bpy)$Cu(CF_3)$] (**1b**) with $ClCH_2CN$ (**2-Cl**) likely proceeds exclusively through a XAT process (pathway D). The following analysis of our experimental and computational data lead to these conclusions.

The experimental observation that both reactions were partially or fully inhibited by the presence of the radical inhibitor TEMPO argues against a concerted pathway for oxidative addition of $BrCH_2CN$ (**2-Br**) to ionic Cu(I) complex $[Ph_4P]^+[Cu(CF_3)_2]^-$ (**1a**) or for oxidative addition of $ClCH_2CN$ (**2-Cl**) to neutral Cu(I) complex [(bpy)$Cu(CF_3)$] (**1b**) (Fig. 4, pathway A). In addition, DFT calculations showed that the computed barrier (42.5 kcal/mol) for oxidative addition of $BrCH_2CN$ (**2-Br**) to complex **1a** through a concerted pathway (pathway A) is much greater than that of the S_N2-type pathway (pathway B; 22.5 kcal/mol) (Fig. 4) or XAT process (pathway D; 23.8 kcal/mol) (Fig. 4). Likewise, the computed barrier (36.3 kcal/mol) for oxidative addition of $ClCH_2CN$ (**2-Cl**) to complex **1b** by pathway A is about 16.0 kcal/mol greater than the lowest-energy alternative pathway, in this case the XAT process (pathway D; 20.3 kcal/mol).

The experimental observation that the addition of SET inhibitor 1,4-dinitrobenzene did not greatly affect either oxidative addition process argues against an OSET pathway (Fig. 4, pathway C). Moreover, the computed barriers for both reactions through an OSET pathway (39.3 kcal/mol and 24.3 kcal/mol, respectively) are 16.8 kcal/mol and 4.0 kcal/mol greater than the S_N2-type pathway A for reaction with complex **1a** or XAT pathway D for reaction

with complex **1b**. Thus, both the experimental and computational data are inconsistent with reaction through an OSET pathway (Fig. 4, pathway C).

By contrast, the relative reactivity of the alkyl electrophiles toward the ionic Cu(I) complex **1a** of ICH_2CN > $BrCH_2CN$ >> $TsOCH_2CN$ >> $ClCH_2CN$ is consistent with an S_N2-type pathway B. In addition, the reaction of the secondary alkyl bromide 2-bromopropionitrile **2-Br-Me** with ionic Cu(I) complex **1a**, which is 1.5 times as slow as that of the less-hindered bromoacetonitrile **2-Br** [$(1.15 \pm 0.01) \times 10^{-3}$ $M^{-1}{\cdot}s^{-1}$ versus $(1.78 \pm 0.03) \times 10^{-3}$ $M^{-1}{\cdot}$ s^{-1}], is inconsistent with OSET or XAT pathways (Fig. 4, pathways C and D). The reaction of a secondary alkyl halide through an OSET or XAT pathway would be faster than that of the primary alkyl halide because of the greater stability of the secondary alkyl radical.

Also consistent with reaction through an S_N2 pathway B, the reactions of complex **1a** with $BrCH_2CN$ (**2-Br**) in polar solvents were faster than those in less-polar solvents, and the more sterically hindered 2-bromopropionitrile **2-Br-Me** reacted more slowly than did **2-Br**. The generation of TEMPO–CH_2CN as a side product from the reaction of complex **1a** with $BrCH_2CN$ (**2-Br**) in the presence of TEMPO suggests that an alternative but minor pathway also occurs during the reaction of the cuprate **1a**. Consistent with this experimental observation, the barrier for a reaction of **1a** with $BrCH_2CN$ (**2-Br**) through a XAT pathway D (23.8 kcal/mol) computed with DFT was only 1.3 kcal/mol greater than that of the S_N2-type pathway B. Furthermore, the calculated barrier (22.5 kcal/mol for S_N2-type pathway B and 23.8 kcal/mol for XAT pathway D) is close to the corresponding experimentally observed activation energy (21.3 kcal/mol), which provides additional evidence to support the proposed mechanism for reaction of **1a** with haloacetonitrile.

Our data for reaction of the neutral copper complex **1b** are more consistent with XAT pathway D as the dominant mechanism. The considerable inhibiting effect of the addition of TEMPO on the reaction of chloroacetonitrile **2-Cl** with [(bpy)Cu(CF_3)] (**1b**) suggests that a free radical •CH_2CN is generated. The barrier for an OSET pathway C computed with DFT (24.3 kcal/mol) is much higher than that of the XAT process (pathway D, 20.3 kcal/mol). In addition, the calculated Gibbs free energy (ΔG; 20.3 kcal/mol) is close to the barrier (18.6 kcal/mol) determined experimentally, implying that a XAT process (pathway D) is the most likely pathway involving an alkyl radical for oxidative addition of alkyl halides to the neutral Cu(I) complex **1b**.

Our experimental and computational data are most consistent with reaction of the alkyl halide directly with [(bpy)Cu(CF_3)] (**1b**). The zero-order dependence on ligand is inconsistent with reversible ligand dissociation followed by oxidative addition (Fig. 4, pathway E). Furthermore, the computed ΔG for dissociation of bipyridine from complex **1b** (17.5 kcal/mol) is accessible, but the computed barrier for a XAT process (pathway D) from $ClCH_2CN$ to the resulting ligandless [$CuCF_3$] is an additional 22.1 kcal/mol. The combination of these energies is much greater than the computed $\Delta G^{\ddagger}$ (20.3 kcal/mol) for direct XAT to **1b** (pathway D).

To gain more insight into the oxidative addition of the haloacetonitrile to Cu(I) complex **1a** and **1b**, we conducted natural population analysis (NPA) on reactants **1a, 1b, 2-Br**, and

2-Cl; transition states **TS-a-S_N2, TS-a-XAT** and **TS-b-XAT**; and products [$L_nCu^{III}(CF_3)(X)(CH_2CN)$] (where L_n is CF_3^- or bpy) (figs. S33 and S35). These studies showed that a small amount of positive charge accumulates on the copper in the transition states (+0.26 for **1a** versus+0.35 for[$Cu^{III}(CF_3)_2(Br)(CH_2CN)]^-$) during the reaction of **1a** with **2-Br** (53, 54) and that the negative charge of the CF_3 moiety decreases considerably (−1.26 for **1a** versus −0.59 for $[Cu^{III}(CF_3)_2(Br)(CH_2CN)]^-$). Even though the change in charge to copper from starting complex to the intermediate after oxidative addition is small, the sum of the negative charge of the bromide and cyanomethyl ligands (−CH_2CN) is large (−0.76 e^-). The same trend was also observed for the reaction of **2-Cl** with **1b**. These changes in charge show that electron density flows from the complexes **1a** or **1b** overall to the haloacetonitriles during the reaction, thus demonstrating that reaction of haloacetonitrile to **1a** or **1b** can be considered an oxidative addition process.

Previous proposals for the mechanism of copper-catalyzed cross-coupling often involve a Cu(I)/Cu(II) redox cycle, on the basis of the experimental evidence for the presence of free radicals, which was typically deduced from quenching experiments with radical scavengers or from racemization or rearrangements of radical clock substrates. Our studies suggest that a free radical could be involved in the oxidative addition of an alkyl halide to Cu (I) to form a Cu(III) intermediate in these pathways through XAT. Oxidative addition of the C(sp^3)–X bond to a Cu(I) species is often considered to be the rate-limiting step of copper-catalyzed cross-coupling reactions of alkyl electrophiles, but studies of this elementary step alone are rare, largely because of the inherent instability of the copper intermediate. Thus, the example of oxidative addition of a C(sp^3)–X bond to Cu(I) in the current study may help develop more efficient copper-catalyzed cross-coupling reactions of alkyl electrophiles.

Supplementary Material

Refer to Web version on PubMed Central for supplementary material.

ACKNOWLEDGMENTS

Funding:

Q.S. gratefully acknowledges financial support from the National Key Research and Development Program of China (2021YFF0701700) and the National Natural Science Foundation of China (22061160465). X-S.X. acknowledges financial support from the National Natural Science Foundation of China (22122104). J.F.H. acknowledges funding from the NIH (R35GM130387). Y. Luo thanks Syngenta for a PhD scholarship.

REFERENCES AND NOTES

1. Beletskaya I, Cheprakov AV, Coord. Chem. Rev. 248, 2337–2364 (2004).
2. Evano G, Blanchard N, Toumi M, Chem. Rev. 108, 3054–3131 (2008). [PubMed: 18698737]
3. Monnier F, Taillefer M, Angew. Chem. Int. Ed. 48, 6954–6971 (2009).
4. Bhunia S, Pawar GG, Kumar SV, Jiang Y, Ma D, Angew. Chem. Int. Ed. 56, 16136–16179 (2017).
5. Cheng L-J, Mankad NP, Chem. Soc. Rev. 49, 8036–8064 (2020). [PubMed: 32458840]
6. Zhou H, Li Z-L, Gu Q-S, Liu X-Y, ACS Catal. 11, 7978–7986 (2021).
7. Dong X-Y et al. Nat. Chem. 11, 1158–1166 (2019). [PubMed: 31636393]
8. Mo X, Chen B, Zhang G, Angew. Chem. Int. Ed. 59, 13998–14002 (2020).
9. Wang FL et al. Nat. Chem. 14, 949–957 (2022). [PubMed: 35618768]

10. Corey EJ, Posner GH, J. Am. Chem. Soc. 89, 3911–3912 (1967).
11. Burns DH, Miller JD, Chan H-K, Delaney MO, J. Am. Chem. Soc. 119, 2125–2133 (1997).
12. Wang G-Z et al. Org. Lett. 17, 3682–3685 (2015). [PubMed: 26181828]
13. Yang C-T, Zhang Z-Q, Liu Y-C, Liu L, Angew. Chem. Int. Ed. 50, 3904–3907 (2011).
14. Su X-L et al. Angew. Chem. Int. Ed. 60, 380–384 (2021).
15. Li C, Chen B, Ma X, Mo X, Zhang G, Angew. Chem. Int. Ed. 60, 2130–2134 (2021).
16. Kainz QM et al. Science 351, 681–684 (2016). [PubMed: 26912852]
17. Chen C, Peters JC, Fu GC, Nature 596, 250–256 (2021). [PubMed: 34182570]
18. Yoshikai N, Nakamura E, Chem. Rev. 112, 2339–2372 (2012). [PubMed: 22111574]
19. Sambiagio C, Marsden SP, Blacker AJ, McGowan PC, Chem. Soc. Rev. 43, 3525–3550 (2014). [PubMed: 24585151]
20. Li S-J, Lan Y, Chem. Commun. 56, 6609–6619 (2020).
21. Ahn JM, Ratani TS, Hannoun KI, Fu GC, Peters JC, J. Am. Chem. Soc. 139, 12716–12723 (2017). [PubMed: 28817770]
22. Lee H et al., J. Am. Chem. Soc. 144, 4114–4123 (2022). [PubMed: 35167268]
23. Hickman AJ, Sanford MS, Nature 484, 177–185 (2012). [PubMed: 22498623]
24. Casitas A, Ribas X, Chem. Sci. 4, 2301–2318 (2013).
25. Liu L, Xi Z, Chin. J. Chem. 36, 1213–1221 (2018).
26. Liu H, Shen Q, Coord. Chem. Rev. 442, 213923 (2021).
27. Bertz SH, Cope S, Murphy M, Ogle CA, Taylor BJ, J. Am. Chem. Soc. 129, 7208–7209 (2007). [PubMed: 17506552]
28. Bertz SH, Cope S, Dorton D, Murphy M, Ogle CA, Angew. Chem. Int. Ed. 46, 7082–7085 (2007).
29. Bartholomew ER et al. Chem. Commun. (10): 1176–1177 (2008).
30. Gärtner T, Henze W, Gschwind RM, J. Am. Chem. Soc. 129, 11362–11363 (2007). [PubMed: 17711285]
31. Brothers PJ, Roper WR, Chem. Rev. 88, 1293–1326 (1988).
32. Shen H et al. J. Am. Chem. Soc. 139, 9843–9846 (2017). [PubMed: 28689419]
33. Paeth M et al. J. Am. Chem. Soc. 141, 3153–3159 (2019). [PubMed: 30678456]
34. Liu S et al. J. Am. Chem. Soc. 142, 9785–9791 (2020). [PubMed: 32365294]
35. Zanardi A, Novikov MA, Martin E, Benet-Buchholz J, Grushin VV, J. Am. Chem. Soc. 133, 20901–20913 (2011). [PubMed: 22136628]
36. Morimoto H, Tsubogo T, Litvinas ND, Hartwig JF, Angew. Chem. Int. Ed. 50, 3793–3798 (2011).
37. Dubinina GG, Furutachi H, Vicic DA, J. Am. Chem. Soc. 130, 8600–8601 (2008). [PubMed: 18543912]
38. Liu H, Shen Q, Org. Chem. Front. 6, 2324–2328 (2019).
39. Martínez de Salinas S et al. Chem. Eur. J. 25, 9390–9394 (2019). [PubMed: 30714647]
40. Tye JW, Weng Z, Johns AM, Incarvito CD, Hartwig JF, J. Am. Chem. Soc. 130, 9971–9983 (2008). [PubMed: 18597458]
41. Tye JW, Weng Z, Giri R, Hartwig JF, Angew. Chem. Int. Ed. 49, 2185–2189 (2010).
42. Isse AA, Gennaro A, J. Phys. Chem. A 108, 4180–4186 (2004).
43. Rendina LM, Puddephatt RJ, Chem. Rev. 97, 1735–1754 (1997). [PubMed: 11848891]
44. Stille JK, Lau KSY, J. Am. Chem. Soc. 98, 5841–5849 (1976).
45. Whitesides GM, Fischer WF Jr., San Filippo J Jr., Bashe RW, House HO, J. Am. Chem. Soc. 91, 4871–4882 (1969).
46. Pearson RG, Gregory CD, J. Am. Chem. Soc. 98, 4098–4104 (1976).
47. Sears JD, Neate PGN, Neidig ML, J. Am. Chem. Soc. 140, 11872–11883 (2018). [PubMed: 30226380]
48. Jones GD et al. J. Am. Chem. Soc. 128, 13175–13183 (2006). [PubMed: 17017797]
49. Diccianni JB, Katigbak J, Hu C, Diao T, J. Am. Chem. Soc. 141, 1788–1796 (2019). [PubMed: 30612428]

50. Fang C et al. J. Am. Chem. Soc. 141, 7486–7497 (2019). [PubMed: 30977644]
51. Matyjaszewski K, Xia J, Chem. Rev. 101, 2921–2990 (2001). [PubMed: 11749397]
52. Novák P, Lishchynskyi A, Grushin VV, J. Am. Chem. Soc. 134, 16167–16170 (2012). [PubMed: 22998369]
53. DiMucci IM et al. J. Am. Chem. Soc. 141, 18508–18520 (2019). [PubMed: 31710466]
54. Shearer J, Vasiliauskas D, Lancaster KM, Chem. Commun. 59, 98–101 (2022).

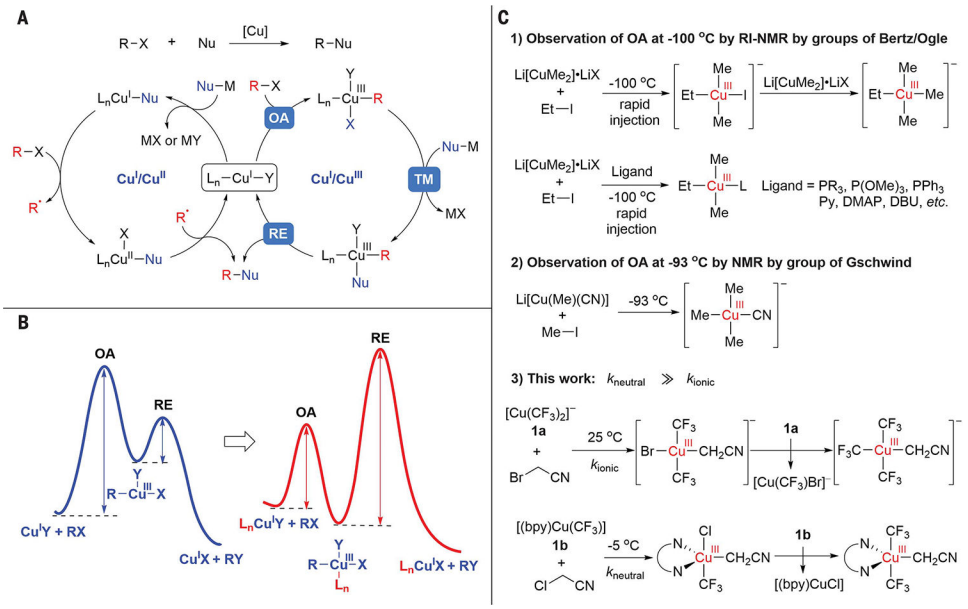

Fig. 1. Mechanism of Cu-mediated cross-coupling.

(**A**) General mechanism for Cu-catalyzed cross-coupling reaction. (**B**) Strategy that inverted the barrier for oxidative addition (OA) and reductive elimination (RE) in the catalytic cycle for Cu-catalyzed cross-coupling. (**C**) State-of-the-art observations of oxidative addition of alkyl halide to Cu(I) species. M, metal or quasi-metal; X, halogen; Y, dummy ligand; TM, transmetalation.

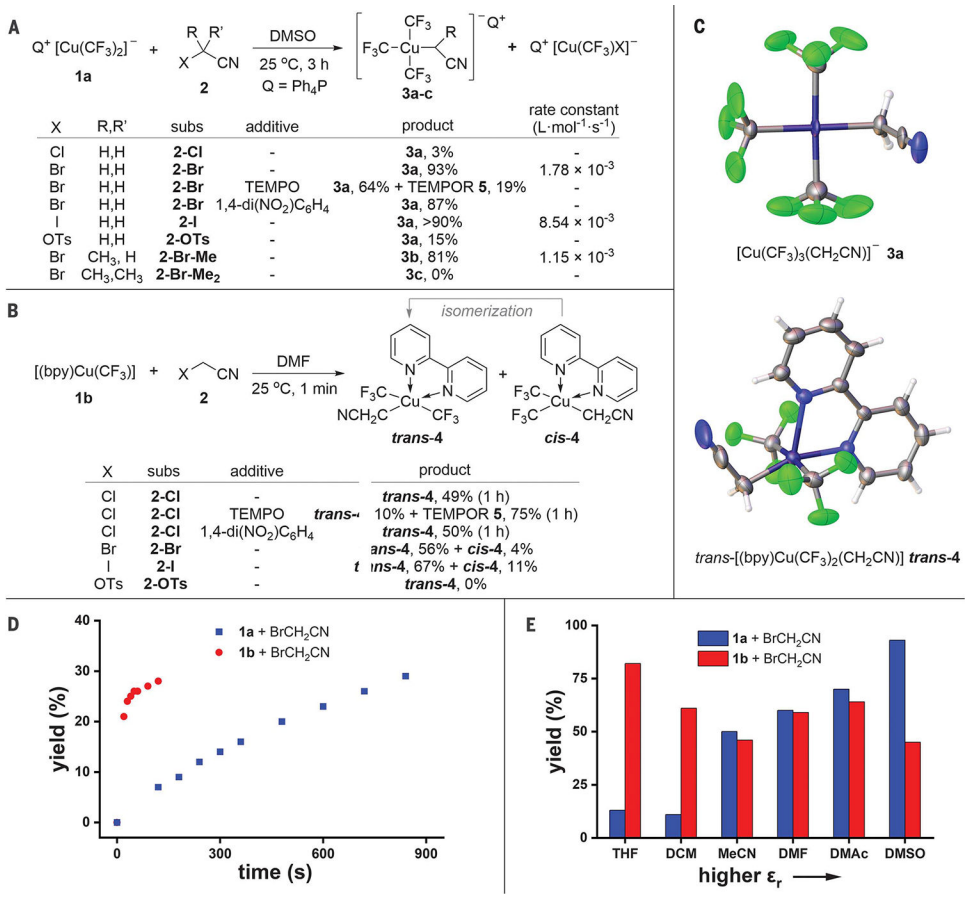

Fig. 2. Oxidative addition of alkyl halides to Cu(I) complexes.

(**A**) Oxidative addition of XCH(R)CN with ionic Cu(I) complex $[Ph_4P]^+$ $[Cu(CF3)2]^-$ (**1a**). (**B**) Oxidative addition of XCH(R)CN with [(bpy)Cu(CF_3)] (**1b**). (**C**) ORTEP (Oak Ridge Thermal Ellipsoid Plot) diagrams of $[Ph_4P]^+$ $[Cu(CF_3)_3(CH2CN)]^-$ (**3a**) (countercation Ph_4P^+ is omitted for clarity) and *trans*-[(bpy)Cu(CF_3)$_2$(CH_2CN)] (***trans*-4**). Ellipsoids are shown at the 50% level. (**D**) Reaction progress for ionic Cu(I) complex $[Ph_4P]^+$ $[Cu(CF_3)_2]^-$ (**1a**) with BrCH2CN (**2-Br**) at 298 K (blue) or neutral Cu(I) complex [(bpy)Cu(CF_3)] (**1b**) with $BrCH_2CN$ (**2-Br**) at 298 K (red). (**E**) Solvent effect on the reactions of $BrCH_2CN$ with $[Ph_4P]^+$ $[Cu(CF_3)_2]^-$ (**1a**) (blue) or [(bpy)Cu(CF3)] (**1b**) (red). DCM, dichloromethane; MeCN, acetonitrile (methyl cyanide).

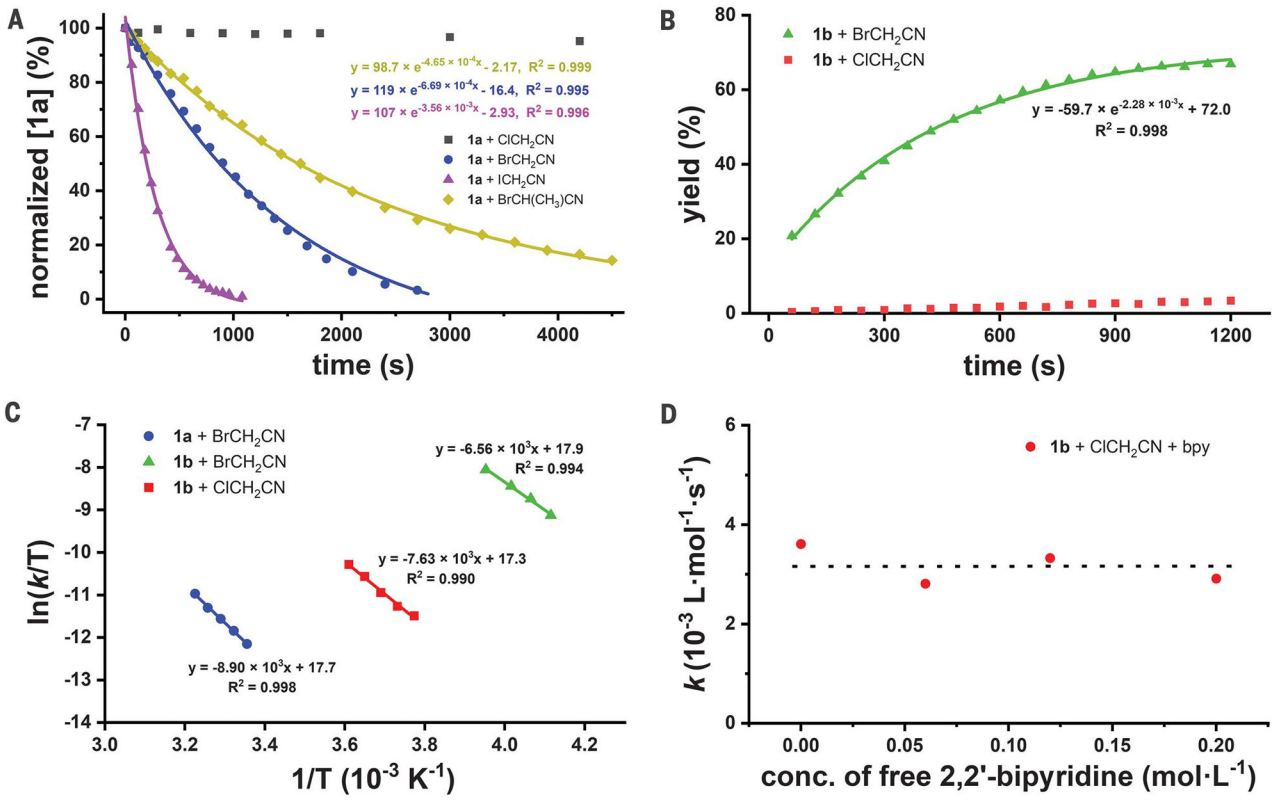

Fig. 3. Kinetic analysis.

Kinetic data were fit to the expression of $[\mathbf{1a}]_t = [\mathbf{1a}]_0 e^{-k_{obs}} + c$ for (A) and $[\mathbf{4}]_t = A - Be^{-k_{obs}}$ for (B), in which t is time and k_{obs} are the apparent (observed) rate constants (pages S12 and S35 to S38 provide details about derivation of expression of corrected rate constant k_{corr} from k_{obs}). (**A**) Kinetic profiles of oxidative addition of XCH(R)CN (where X is Cl, Br, or I; and R is H or Me) with ionic Cu(I) complex $[Ph_4P]^+[Cu(CF_3)_2]^-$ (**1a**) at 298 K. (**B**) Kinetic profiles of oxidative addition of XCH_2CN (where X is Cl or Br) with [(bpy)Cu(CF_3)] (**1b**) at 243 K. (**C**) Eyring analysis of the temperature dependence of the rate constants of oxidative addition of $BrCH_2CN$ with $[Ph_4P]^+[Cu(CF_3)_2]^-$ (**1a**) (blue), oxidative addition of $BrCH_2CN$ with [(bpy)Cu(CF_3)] (**1b**) (green), and oxidative addition of $ClCH_2CN$ with [(bpy)Cu(CF_3)] (**1b**) (red). (**D**) Effect of added free bipyridine on oxidative addition of $ClCH_2CN$ with [(bpy)Cu(CF_3)] (**1b**) at 268 K.

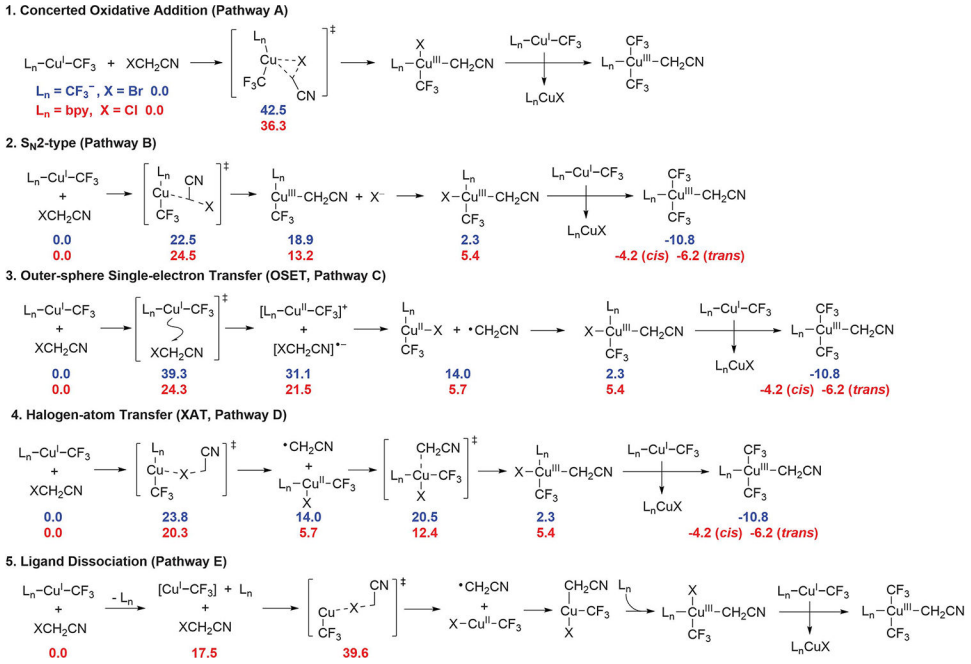

Fig. 4. Five proposed pathways for the oxidative addition of haloacetonitriles to ionic or neutral Cu(I) complexes and free energies of each species computed with DFT.

The calculated activation free energies for the oxidative addition of $BrCH_2CN$(**2-Br**) to the ionic Cu(I) complex $[Ph_4P]^+$ $[Cu(CF_3)_2]^-$ (**1a**) in DMSO are given in blue, and those for oxidative addition of $ClCH_2CN$ (**2-Cl**) to the neutral [(bpy)Cu(CF_3)] (**1b**) in DMF are given in red. The energies are in kilocalories per mole and indicate the relative free energies calculated at the PBE0-D3(BJ)/Def2-TZVP(SMD, solvent)//PBE0-D3(BJ)/Def2-SVP(SMD,solvent) level. SMD, solvation model density.